bSlight 2.0: Battery-free Sustainable Smart Street Light Management System

Prajnyajit Mohanty, *Graduate Student Member, IEEE*, Umesh C. Pati, *Senior Member, IEEE*, Kamalakanta Mahapatra, *Senior Member, IEEE* and Saraju P. Mohanty, *Senior Member, IEEE*

Abstract—Street lighting is one of the prominent applications that demand a massive amount of power and substantially contributes to the energy budget of a country. Light Emitting Diode (LED) and the advancement of Internet of Things (IoT) have significantly improved conventional street light technology. Nevertheless, the rapid growth of IoT devices has presented a formidable challenge in powering the vast array of IoT devices. In this manuscript, a sustainable, battery-free, low-power street light management system has been proposed which is powered from hybrid solar and solar thermal energy harvesting scheme integrated with an efficient power management unit. As a specific case study, the prototype has been implemented with an existing LED street light in India. The characteristics and performance of the prototype have been evaluated to ensure its seamless operation under real-world scenarios. The average power consumption of the system is measured as 2.088 mW when operating in real-time with 50% duty cycle, exhibiting high Quality of Service (QoS). It features long-range communication up to 761 m through implementing LoRaWAN technology. Dimension of the prototype has been restricted to 10.5 cm x 6.5 cm x 2.3 cm to make it suitable for retrofitting with existing LED based street lights.

Index Terms—Smart Energy, Sustainability, Street Light Management, Energy Harvesting, Solar Energy, IoT, LoRaWAN, Smart Cities

1 Introduction

The rapid advancement of technology has ushered significant transformation in various aspects of human life. This revolution has undeniably exerted a significant and positive influence on society, leading to numerous developments. Street lighting is an application that has a profound impact on day to day life of human beings. It is considered to be one of the most energy consuming application in smart city aspect as it accounts for 30% – 40% of the total energy budget of a city [1]. Thus, energy efficiency is a crucial consideration in the design of public lighting systems. Light Emitting Diode (LED) based lights have been used as a replacement for traditional incandescent street lights in order to enhance energy efficiency. Further, unceasing efforts have been made in this direction by incorporating Internet of Things (IoT) technology in the recent past. The framework of IoT enabled smart street light management system is depicted in Fig. 1. However, the proliferation of IoT nodes has experienced exponential growth due to its extensive uses across various applications. As a result, the number of IoT nodes around the globe is projected to surpass 30 billion by 2025 [2]. The IoT nodes are powered by either primary or secondary batteries. Replacement or recharging these batteries is not a practical or economically suitable solution. Supplying energy to such massive number of IoT nodes has surfaced as a formidable issue, which may slow down the wide adoption of IoT globally. As a result, this acts as an impetus to develop battery-free, sustainable IoT devices complying with Sustainable Development Goal (SDG) 9 of United Nations (UN) [3]. On the other hand, integrating sustainability to IoT devices deployed in a wide range of application has emerged as a new research challenge for researchers [4]. Powering IoT devices from renewable energy sources, including but not limited to solar, wind, thermal, mechanical vibration, and radiofrequency, to bring energy sustainability has become a viable solution. Solar energy exhibits superior power density and output voltage in comparison to alternative energy sources [5]. It is a highly favoured energy source for various outdoor applications due to its widespread availability.

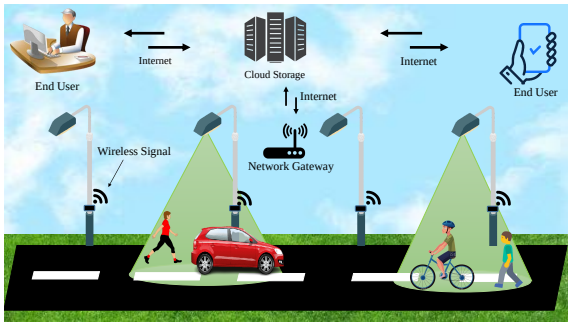

Fig. 1. Smart street light management system

1.1 Related Prior Work

Numerous developments have been conducted in the past on designing and developing smart street light management systems. Street lights are featured with dimmable capability and weather adaptive conditions in [9] – [11], respectively. The light intensity of street lights has also been dynamically controlled by implementing the Artificial Bee Colony

- *P. Mohanty, U. C. Pati, K. K. Mahapatra are with Department of Electronics and Communication Engineering, National Institute of Technology Rourkela, India.*
  E-mail: prajnyajitmohanty@gmail.com, ucpati@nitrkl.ac.in, kkm@nitrkl.ac.in.
- *Saraju P. Mohanty is with Department of Computer Science and Engineering, University of North Texas, Denton, TX.*
  E-mail: saraju.mohanty@unt.edu

Manuscript is submitted on 28 Nov. 2023.

(ABC) algorithm in [14]. In [16], an intelligent street light management system has been proposed that can detect various objects by using advanced image processing and Artificial Intelligence (AI) techniques to precisely control the brightness of the light. Communication system is a major part of designing smart street light management systems. In [17] and [18], ZigBee has been used to communicate the street light data in short-range. Further, General Packet Radio Service (GPRS) communication technology has also been integrated with ZigBee in [19] to feature high communication range. However, it has also been observed from the literature that the integration of GPRS leads to an escalation in power consumption. Further, Wireless Fidelity (WiFi) is incorporated in [20] with street lights, which consume less energy and feature long-range communication in street light management system to control the illuminance of street lights. Digital Addressable Lighting Interface (DALI) protocol has been used in [15] to bring cost-effectiveness in smart street light management system. In [22], a cloud-based street light management system has been designed with dedicated security features. In [23], a smart IoT-based LED lighting system has been proposed and implemented for office environments, which has been proven to be energy efficient. In [24], fuzzy logic based flexible and adjustable control system has been proposed for controlling the intensity of light.

In the recent past, a number of energy-efficient LoRaWAN-based systems have been developed. LoRaWAN based health monitoring solution for soldiers has been proposed in which attempts have been made to increase the reaction time of the system to deploy it in emergency applications [25]. Furthermore, an energy-efficient smart metering system using edge computing in LoRa is presented in [26]. LoRaWAN has been implemented in various solar energy powered IoT systems deployed in real-time in [27] – [29]. Subsequently, LoRaWAN has also been used in batteryless energy autonomous quality monitoring system [30]. The optimization of solar cell size, energy storage unit, and energy requirement are crucial aspects in the design of solar energy powered systems, which is discussed in [31].

1.2 Issues in the existing works and proposed solution

The design and implementation method of street light management system has been the subject of ongoing research and development. However, it is important to note that several significant issues have been identified in the existing works. The issues and the proposed solutions are highlighted below.

1.2.1 The necessity of sustainability in street light management system

It has been observed from the literature review that there are two ways to power the existing street light management systems, i.e., battery or direct AC supply from the street light using AC-DC converter. The growing number of batteries has turned to be an issue due to their adverse impact on the environment, prompting measures to limit their use. Powering street light management systems from direct power available in grid-connected street lights has been reported to be a feasible option in smart cities and urban areas [8], [9]– [11], [13]– [15]. However, remote areas, such as hilly regions, deserts, and villages lacking a grid network, pose a significant challenge in this case. Consequently, standalone/split-type solar street lights have become a viable solution and are widely deployed in these regions. Though standalone solar street lights are incorporated with LED which makes them energy-efficient, all-in-one solar street lights are proven more energy efficient and feasible due to their smart features as well as management system. Estimating or stating the exact number of standalone solar street lights deployed globally is challenging. According to report of Ministry of New and Renewable Energy (MNRE), 9 lakh standalone solar street lights have been installed in india by 2021 under off-grid and decentralized solar application scheme [32]. Hence, it is essential to enhance energy efficiency in such a vast number of standalone solar street lights. The primary possible way of providing smart features to the installed standalone solar street lights is to integrate them with state-of-the-art smart street light management systems, which implies the fulfillment of the power demand of the street light management system by the Photovoltaic (PV) panels of standalone solar street lights. This allows standalone solar street lights to work similar to an all-in-one solar street light. However, this method has considerable drawbacks including the following.

- The existing street light management systems are typically power hunger devices. The power consumption of the device must be optimized and maintained at minimum to integrate it with the PV panel of the street light.
- The size and output power of PV systems in street lights are designed and optimized considering the consumption of load, specifically lighting duration; thus, implementation of the aforementioned approach may disturb design equation of the solar powered street light, causing power failure in it.
- The entire existing street light infrastructure, including PV panels, associated electronics, and batteries, has to be replaced in this approach, which may not be preferred as a cost-effective way.

Thus, the proposed system has its dedicated energy harvesting sub-system intended to supply and manage its power, making it completely self-sustainable. The average cost of a standard commercial all-in-one solar street light which can be deployed to highways is 150$ to 800$. The approximate manufacturing cost of the proposed system is much less than half of the aforementioned price. It offers the potential benefit of retrofitting not only with standalone solar street lights but also with grid-powered street lights, and hybrid-powered street lights to bring energy efficiency. This in turn, makes it suitable for implementation with existing street light infrastructure not only in rural and remote places such as hilly regions, deserts, and villages but also in smart cities.

1.2.2 Energy harvesting, and battery-free design

The major energy requirement of the device is during night when energy availability is extremely critical. The feasibility of energy harvesting from artificial light has been investigated in [6], which is used as the primary energy source as the device is intended to work full-fledged during

night. Sunlight possesses far higher power density compared to artificial light, and the recent advancements in PV technologies ensure energy harvesting at high efficiency from sunlight. However, the harvested energy during day hours can not be stored in supercapacitors due to their low energy density unlike batteries. Thus, uninterrupted energy harvesting is highly essential in this system to overcome the issue of low energy density of supercapacitor. Subsequently, the power density of artificial light is much lower than sunlight, and adverse weather conditions such as fog, and heavy rain may hinder issues in energy harvesting causing potential chance of power failure in the system. This issue can be solved by incorporating an energy buffer with the device which can supply power during adverse environmental condition providing capability to the device to sustain its operation when uninterrupted energy harvesting is difficult. Batteries are the mostly opted energy storage element to meet this design requirement due to its low cost and high availability. However, designing a battery-free system meeting the above mentioned design requirement is critical. In the proposed work, a hybrid energy harvesting scheme has been implemented which can harvest solar energy and solar thermal energy during presence of sunlight. Lithium-ion capacitor has been used to store energy which possess adequate power as well as energy density promoting green IoT paradigm.

1.2.3 Optimization of power consumption

The existing systems are predominantly focused on enhancing the features in street light management systems. Nevertheless, power consumption of the system increases with the increase in number of features, which has not been addressed in the state-of-the-art solutions. On the other hand, optimization of power consumption has been of the utmost importance in designing energy-autonomous devices. It has been optimized using duty cycle optimization technique in most of the energy-autonomous devices [27] – [29], [30] due to its ease of implementation. However, Quality of Service (QoS) is a significant issue due to low duty cycle of operation in these systems. In order to provide the necessary QoS, solar energy powered energy autonomous systems used in the outdoors incorporate larger-sized solar cells with output power in few watts and surface area of more than 100 cm^2 [33], [34]. The size of the device which is considered as a crucial design metric in IoT technology, emerges as a significant concern in those cases. In this work, duty cycle technique has been used to optimize the power consumption of the device. Subsequently, attempts have been made to uphold high percentage of duty cycle of operation to ensure high QoS while keeping the harvester size smaller. It has been achieved by prioritizing the tasks as per the requirements of the application and implementation of high efficient mono-crystalline type solar cell.

1.3 Novel Contribution of Proposed work

The proposed work possesses the following novelty over the existing works.

- In this manuscript, a novel solar and solar thermal energy powered battery-free sustainable street light management system has been proposed which can be readily implemented with any existing LED based street light. It works in real-time to manage the operation of street light in energy efficient way. To the best of our knowledge, this is the first lithium-ion capacitor based street light management system.
- The proposed device is incorporated with a hybrid solar and solar thermal energy harvesting scheme integrated with an efficient energy management system. The power management unit has ability to concurrently store energy in lithium-ion capacitor and power the sensor node through a capacitor, exhibiting the potential of the device to manage energy effectively.
- The power consumption of the sensor node has been optimized to be the minimum compared to the state-of-the-art street light management systems.
- The system demonstrates the potential to operate in real-time with 50% duty cycle, which is more than triple compared to most of the existing solar powered LoRaWAN based energy autonomous systems. Though having such higher percentage of duty cycle, the device is incorporated with smaller size harvesters, which confers an edge to minimize the physical size of the device, rendering it suitable for integration with any street light.
- The proposed device is portable and affordable. It is compatible for seamless integration with the existing LED based street light infrastructure ensuring its high adaptability. This is the most considerable added advantage of the system, making it readily implementable to solar powered, grid-powered and hybrid powered street lights. It can be specifically suitable to standalone solar street lights deployed in smart cities or urban areas, rural and geographically remote areas such as hilly area, and desert. The proposed IoT enabled device is sustainable, low-cost, and requires ultra-low maintenance, demonstrating *plug and forget* feature promoting SDG 7 and SDG 9 of UN [3].

This paper is organized as follows: The overview of the proposed system has been discussed in Section 2. Section 3 presents the experimental set up, prototyping, results and analysis. The manuscript has been concluded in Section 4.

2 Proposed Design Overview

The proposed system has been meticulously designed by integrating cutting-edge techniques for harnessing ambient solar and solar thermal energy, utilizing state-of-the-art low-power electronics, and implementing duty cycle optimization technique for achieving low-power consumption of the hardware. Fig. 2 illustrates the block diagram of the proposed system. The proposed system is further broken down into the following subunits.

2.1 Power Management Unit

The function of Power Management Unit (PMU) includes harnessing solar energy, optimizing the harvested power, storing the energy, and regulating the output voltage of the storage element according to the desideratum of the sensor node. The unit incorporates a small mono-crystalline solar cell of surface dimension 4.2 cm x 2.3 cm and a Thermoelectric generator (TEG) of surface dimension 4.2 cm

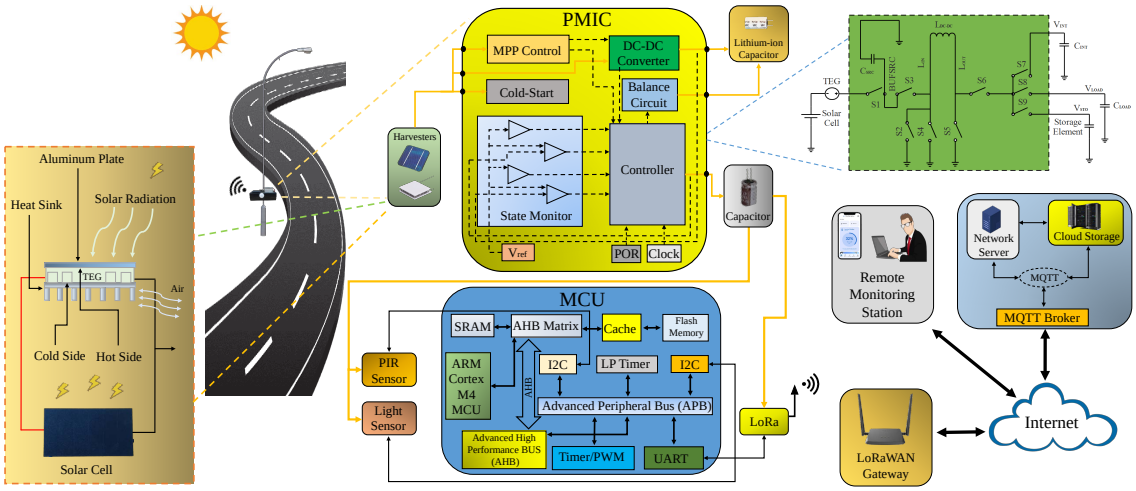

Fig. 2. Block diagram of the proposed system architecture

x 3.8 cm connected in series. The total energy harvested can be calculated using Eqn. (1).

$$\int_{T_1}^{T_2} P_{harv}dt = \int_{T_1}^{T_2} P_{pv}dt + \int_{T_1}^{T_2} P_{TEG}dt \tag{1}$$

where P_{pv} and P_{TEG} represent the output power of the solar cell and TEG, respectively. The solar cell exhibits maximum voltage (V_{pv}^{oc}) of 4.15 V and current (I_{pv}^{sc}) of 58.60 mA as per the manufacturer of the harvester. Subsequently, TEG is capable of harvesting energy based on seebeck effect. The open-circuit voltage generated from TEG (V_{TEG}^{oc}) depends upon the seebeck coefficient (α_{hc}) and temperature difference between the hot side and cold side of the harvester (ΔT). This can be mathematically expressed as below Eqn. (2).

$$V_{TEG}^{oc} = \alpha_{hc} \times \Delta T \tag{2}$$

α_{hc} can be further expressed mathematically as following expression:

$$\alpha_{hc} = \alpha_{hs} - \alpha_{cs} \tag{3}$$

where α_{hs} and α_{cs} represent the seebeck coefficient of hot side and cold side, respectively. ΔT can be calculated following Eqn. (4).

$$\Delta T = T_{hs} - T_{cs} \tag{4}$$

T_{hs} and T_{cs} present the temperature of hot side and cold side of the TEG, respectively. TEG yields V_{TEG}^{oc} of 0.97 V and current (I_{TEG}^{sc}) of 225 mA at ΔT $\approx$ 20°C as per the manufacturer. Subsequently, maximum power from solar cell P_{pv}^{max} can be calculated as follows:

$$P_{pv}^{max} = FF \times V_{pv}^{oc} \times I_{pv}^{sc} \tag{5}$$

where FF denote the fill factor of solar cell. Further, P_{TEG} can be expressed following Eqn. (6).

$$P_{TEG} = Q_{hs} - Q_{cs} = I_{TEG}(\alpha_{hc}\Delta T - I_{TEG}R_{int}) \tag{6}$$

where Q_{hs} and Q_{cs} denote the heat transfer rate from hot side and cold side, respectively. I_{TEG}, and R_{int} represent output current and internal resistance of TEG, respectively.

These harvesters can harness energy during presence of sunlight only, thus the device must satisfy the below expression to avoid power failure.

$$\int_{T_1}^{T_2} P_{harv}dt \ll E_{storage} \tag{7}$$

where $E_{storage}$ represents the energy storing capacity of the storage element based on its energy density. Capacitors and supercapacitors fail satisfying the aforementioned requirement owing to poor energy density. In contrast, lithium-ion capacitors are greener than batteries and have 20 times the energy density of supercapacitors. Thus, it is selected as the primary energy storage element in this work. Further this unit consists of a full-featured energy efficient Power Management Integrated Circuit (PMIC), which functions along with the below subunits in order to achieve its full objective.

- DC-DC Converter: It works in boost configuration in this work. It boosts the input voltage from the source (V_{src}), which ranges from 0 V to 4.15 V at open circuit conditions. The converter boosts the voltage at BUFSRC, which typically establishes a connection with an external capacitor to buffer the input of the DC-DC converter or at STO to a level suitable for charging the storage element STO or to regulate the LOAD and the internal supply V_{INT}. The converter has switching transistors such as S2 or S3, S4, S5, and S6. The controller selects LOAD, STO and V_{INT} through S7, S8, and S9, respectively. The converter has two inputs such as BUFSRC or STO, and the default input is BUFSRC through S3. In the event that the energy provided by the SRC is insufficient to sustain the desired voltage levels of LOAD or V_{INT}, the converter uses STO as an alternative input via M2 in order to maintain the regulation of LOAD and V_{INT}.
- Cold Start: The PMIC commences cold start process promptly upon reaching the necessary voltage threshold of 275 mV. It is imperative that a minimum input power (P_{SRC}) of 3 μW is present at the source to facilitate this startup. Following the cold start, the PMIC can start

extracting power from the source subject to minimum V_{SRC} of 100 mV.

- Maximum Power Point Tracking (MPPT) control: It assesses V_{MPP}, which represents the optimal voltage at which the energy source delivers its maximum output power. The PMIC provides a range of selectable Maximum Power Point (MPP) ratio from 0.6 to 0.9, sampling period from 280 ms to 71.7 sec and sampling duration in the range of 5.19 ms to 1.12 sec.
- State Monitor: It monitors various PMIC states, which plays a vital role in its operation. The primary function of state monitor is to execute various operation states. In addition to that it safeguards the storage element from potential damage caused by excessive charging or discharging. The PMIC protects the storage element from over-charging and over-discharging by continuously monitoring and comparing V_{STO} with over-charging voltage threshold (V_{ovch}) and over-discharging voltage threshold (V_{ovdis}). It interrupts the power flow to the storage element in the event of excessive charging while also initiating a shutdown during excessive discharging.
- Controller: It performs all the necessary control actions coordinating with other subunits of PMIC to execute various operations including DC-DC convertion, state management, cold start, and MPPT.

The PMIC supports the charging of a pair of energy storage elements. In this work, a lithium-ion capacitor of 150 F along with a supercapacitor of 300 μF have been used as energy storage elements. The PMIC can also provide a selective constant supply voltage (V_{load}) ranging from 1.39 V – 4.65 V to the sensor node for its efficient operation at a stable input supply. This ensures optimal functionality of the sensor node by maintaining a stable input supply. Consequently, the need for an additional Low Dropout (LDO) regulator is obviated, unlike [6], thereby conferring a distinct advantage.

2.2 Sensor Node and Gateway Node

This unit is employed for sensing, controlling, and data communication. The sensor node is designed to sense two parameters such as motion and light intensity. An energy-efficient, low-power microcontroller has been incorporated as the Micro Controller Unit (MCU) of the sensor node. It is an ARM Cortex M4 based high performance microcontroller designed dedicatedly for low-power applications. It takes the input from the ultra-low-power Passive Infrared (PIR) sensor and sends a Pulse Width Modulation (PWM) based control signal to the street light through the AC dimmer module. Further, the light intensity of the street light can be measured using an energy-efficient light sensor. The light sensor can operate in different energy-saving modes to reduce its power consumption. The microcontroller receives the input from the light sensor to ensure the normal operation of the street light. LoRaWAN technology has been implemented for efficient and reliable data communication purposes. The microcontroller sends the working status of the street light to the LoRaWAN gateway. The microcontroller transmits the operational state of the street light to the LoRaWAN gateway through LoRa transceiver. It exhibits communication range of up to 761 m in outdoor environment in this work. LoRaWAN gateway has been used as a node to communicate with the sensor node and send the recieved data to the cloud server through Message Queuing Telemetry Transport (MQTT) broker.

2.3 Remote Monitoring Station

The primary function of this block is enable the admin to check the details of the street light from a remote location. It receives data from the LoRaWAN gateway though internet. The cloud storage unit stores data received from the sensor node. It is enabled with cloud analytics feature which results useful comprehensive insights related to the operation of the street light. It helps admin to keep track of the data from the sensor node. It also offers a Graphical User Interface (GUI) for remote monitoring. The admin can access the data using web portal and mobile application.

2.4 Energy Efficient Firmware

The software algorithm of bSlight 2.0 is shown below. It is programmed to perform efficiently and consumes less energy to achieve its tasks. Duty cycle optimization technique is implemented for its operation, which enables the sensor node to keep the required component in active mode and others in sleep mode to reduce power consumption. It starts its operation by sensing the light intensity and comparing it to a threshold L_{int1} to determine whether it is a day or night. Thus, the sensor node features automatic on-off depending on ambient light intensity. It can be noted that the sets of tasks are different during day and night for the sensor node. It continuously monitors the occupancy precisely vehicles and pedestrians around the road and adjusts the illuminance of the street light at either 100% if occupancy is detected or 50% in case of empty road. Subsequently, it can check the working status of the street light by sensing its light intensity in every 15 minutes. It is often noticed that street lights frequently fail to emit

Algorithm 1: Pseudo Code of Power-Aware Firmware of bSlight 2.0

```
Measurement of light intensity "L_int1"
if L_int ≤ L_1 then
    Turn on the street light
    Detect occupancy
    if Occupancy is detected then
        Generate PWM signal to set illuminance level of light at 100%
    end
    else
        Generate PWM signal to set illuminance level of light at 50%
    end
    if Is it 900 secons? then
        Set illuminance level of light to 100%
        Measurement of light intensity "L_int2"
        if L_int2 ≥ L_2 then
            Satus = Normal
        end
        else
            Status = Abnormal illuminance, needs repair
        end
        Configure LoRa by setting frequency, SF, and CR
        Packetize data
        Transmit L_int2 and Status
        LoRa and light sensor goes in deep sleep mode
    end
end
else
    LoRa, light sensor goes in deep sleep mode and MCU goes in sleep
      mode for 900 seconds
end
return 0
```

their designated brightness level, which might lead to traffic accidents. Hence, the sensor node measures the luminous intensity at a maximum level of 100% to determine the functionality of the street light by comparing it to a threshold value of L_{int2}. Subsequently, it sends the working status to the LoRa gateway. Afterward, it puts LoRa and the light sensor into a deep sleep state for 900 seconds. The GUI makes it convenient for the admin to visualize the working status of each street light and find the faulty one.

3 Experimental Validation

The system has been deployed on field and it's performance has been rigorously validated through experimental analysis. Operational characteristics of the device has been comprehensively presented below.

3.1 Experimental Testbed Setup

The component details of the proposed system has been presented in Table 1. In the process of hardware setup, it is essential to configure the PMIC according to the requirements of the application adhering to the datasheet of manufacturer [35].

TABLE 1
Component details and cost estimation

Component	Part	Key Specification	Cost (USD)
Solar cell	SM141K06L	Maximum output: 184 mW	4
TEG	SP1848	Maximum Temperature: 150°C	2
PMIC	AEM10330	Input: 0.275 – 4.5 V	4.26
Lithium-ion capacitor	VEL13253R8157G	Capacitance: 150 F	9
Capacitor	Electrolytic type	Capacitance: 300 μF	0.2
PIR sensor	EKMB1103111	Range: 12 – 14.5 m	9
MCU	STM32L476	Architecture: ARM cortex M4	8.19
Light sensor	VEML7700	Range: 0 – 120 klx	9.9
Wireless module	RFM95	LoRa	15.57
PCB, Wiring, and Soldering			1.5
Approximate cost of manufacturing			63.62

Fig. 3 presents the configuration of PMIC in the proposed work. There are two parameters to set the MPPT of the PMIC, which are MPP ratio (R_MPP) and MPP timing (T_MPP). R_MPP is configured to 70% by connecting $R\_MPP[2:0]$ pins to binary value 010. $T\_MPP[1:0]$ is configured to 00, which implies that the PMIC performs the necessary MPP calculation continuously, specifically every 341 ms, to optimize the energy harvesting as per the manufacturer.

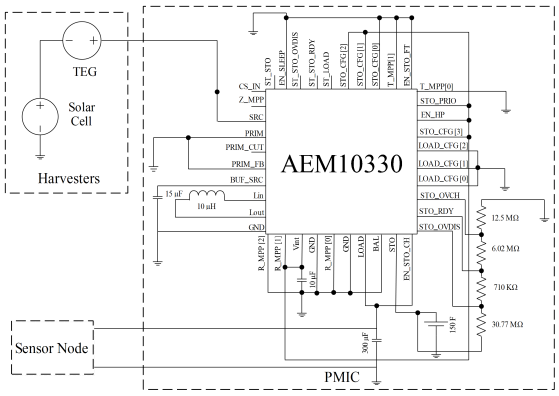

Fig. 3. Configuration of PMIC in bSlight 2.0

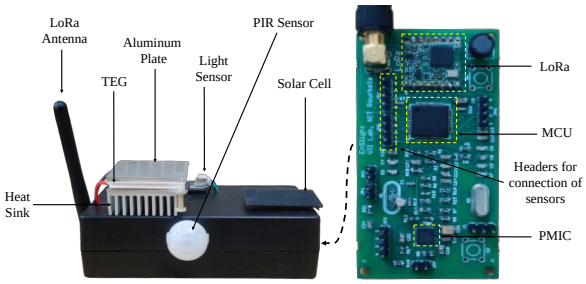

Fig. 4. The fabricated PCB and outer casing of the prototype

Subsequently, two types of storage elements having two different functionalities are used in this work. In order to set up the lithium-ion capacitor, $STO\_CFG[3:0]$ have been configured to 1110 along with the resister bridge connected to STO_OVCH, STO_RDY, and STO_OVDIS pins as shown in Fig. 3 to set V_{OVCH}, V_{RDY} and V_{OVDIS} at 4 V, 2.7 V and 2.6 V, respectively. Further, $LOAD\_CFG[2:0]$ is

(a) (b)

Fig. 5. bSlight 2.0 installed with a LED street light and controlling the illuminance (a) Illuminance is 100% upon detection of pedestrian (b) Illuminance is 50% in empty road

set to 00 such that the sensor node receives power between 3.15 V and 3.34 V. Few additional settings must be tuned in the PMIC for effective energy management. EN_SLEEP is grounded to ensure that the PMIC works in active mode irrespective of time. EN_HP is pulled high to enable the PMIC to maximize its current extraction capability from the

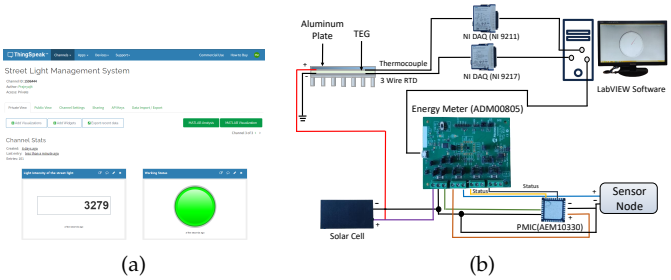

(a) (b)

Fig. 6. (a) GUI showing the working status and illuminance level of light sensor in real-time when illuminance is 100% during remote monitoring (b) Block diagram of experimental measurement setup of the device on field

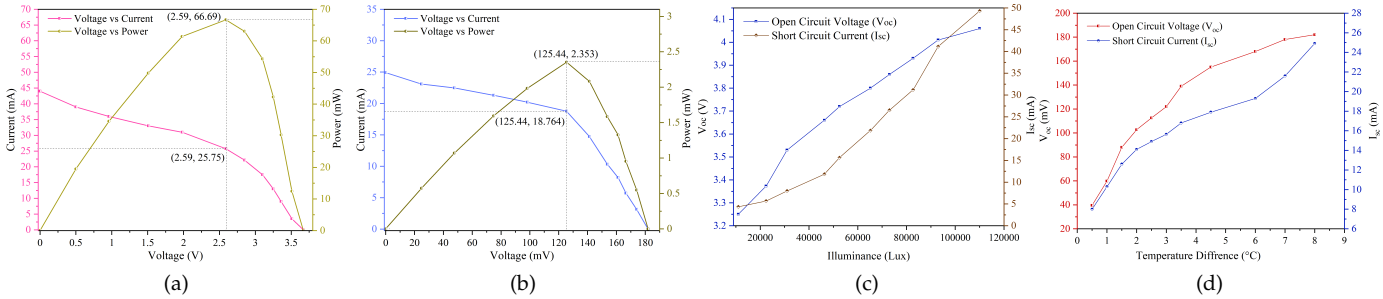

Fig. 7. (a) VI characteristics of solar cell at irradiance of 886 W/m^2 (b) VI characteristics of TEG at ΔT $\approx$ 6°C (c) Open circuit and short circuit characteristics of solar cell (d) Open circuit and short circuit characteristics of TEG

harvesters. Subsequently, EN_STO_CH is set to $LOAD$ to ensure the charging of lithium-ion capacitor. The device gives lithium-ion capacitor the highest charging priority with STO_PRIO set to high value, charging it to a safe limit before supplying power to the sensor via the capacitor connected to $LOAD$. The device has been enclosed within a protective silicon casing as depicted in Fig. 4 in a satisfactory form factor of 10.5 cm x 6.5 cm X 2.3 cm. The device has been deployed with an existing LED based street light as shown in Fig. 5 to test its performance. The data communiacted from the end device is monitored though the developed cloud GUI as shown in Fig. 6(a). The schematic of the experimental setup for measurement of temperature, power, current consumption and energy consumption has been illustrated in Fig. 6(b).

3.2 Electrical Characteristics of the Harvesters

The VI characteristics of the solar cell and TEG have been observed to obtain MPP ratio in experimental condition. The results related to this have been shown in Fig. 7. It can be noted that P_{pv}^{max} is experimentally found to be 66.69 mW at 886 W/m^2. At this condition, open circuit voltage of solar cell (V_{pv}^{oc}) is measured as 3.67 V and the MPP is observed to be 70.57%. Subsequently, P_{TEG}^{max} is observed to be 2.353 mW at ΔT $\approx$ 6.5°C. The measured V_{TEG}^{oc} is 182 mV and the MPP is calculated as 68.92% at this point. Though, ΔT exhibits fluctuations within the range of 0°C to 8°C throughout the day. The average ΔT is observed as 6.5°C during 11 AM to 3.30 PM in summer season. Further, the open circuit

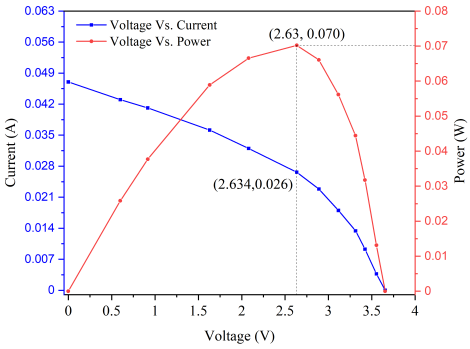

Fig. 8. VI characteristics of harvesters connected in series

characteristics of solar cell and the TEG have been reported in Fig. 7 during a range of illuminance level and ΔT to understand the maximum amount of output power both the harvesters can provide to the sensor node. Subsequently, the VI characteristics of both the harvesters connected in series have been presented in Fig. 8. The observed MPP attained within the experimental conditions amounts to 70.86%.

3.3 Efficient Power Management

The power management system of bSlight 2.0 plays a pivotal role in the accumulation and provision of energy to the sensor node. In this work, the PMIC is an advanced power management circuit that excels in optimising energy efficiency. It primarily offers a highly efficient regulated switching DC-DC converter ensuring optimal power conversion capability. It works in boost configuration in this work. The PMIC can operate through a comprehensive set of seven independent states, each serving a specific purpose. These states include reset state, wake-up state, start state, supply state, sleep state, shutdown state, and primary battery state. The system is completely battery-free, and the PMIC is configured to work in active mode to ensure an uninterrupted power supply to the sensor node. Thus, the PMIC carries out all operational states except the sleep state and the primary battery state in this work. The operational states of the PMIC subject to specific conditions has been shown in Fig. 9(a). The performance of the PMIC has been meticulously examined and analysed in three scenarios. It initiates its operation upon the detection of solar irradiance. It remains in reset state untill minimum P_{SRC} of 3 μW is achieved, after which it starts harvesting energy. The initial process subsequent to the reset state is commonly referred to as the cold start operation. The experimental findings pertaining to the cold start operation is depicted in Fig. 9(b). It can be observed that at 908 seconds since the experiment gets started, P_{SRC} reaches 3.01 μW, and V_{SRC} has been measured as 273 mV at this point. The internal voltage of the PMIC, denoted as V_{Int}, exhibits a gradual rise until it reaches its peak value of 2.2 V. Subsequently, the PMIC transits into start state and delivers energy to the storage element. V_{SRC} is not constant despite appearing as constant in Fig. 9(b). It appears so due to the experimental time frame being limited to 1550 seconds.

Furthermore, V_{Load}, is reported to be 0 V since V_{SRC} is lower than V_{chrdy}. This test has been conducted during early morning 6 AM and ΔT has been measured as 0°C at this time implying $P_{TEG} \approx 0$. Therefore, the energy harvested

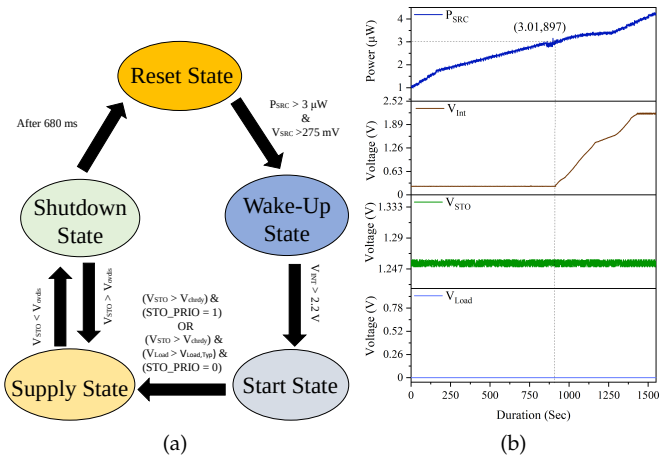

Fig. 9. (a) Flow-chart of operational states of the PMIC (b) PMIC initiating cold start operation on availability of sunlight in the early morning 6 AM

from solar cell is solely contributing towards P_{SRC} in this case. Further, after cold start, the PMIC avails more energy from the source, and the harvested energy gets stored in the storage element, implying a noticeable rise in V_{STO}. Thus, it starts working in start state and supply state. Fig. 10(a) illustrates the operation of PMIC during both these states. It has been experimentally observed that the TEG exhibits a gradual increase in its contribution to P_{SRC} in conjunction with the solar cell during supply state.

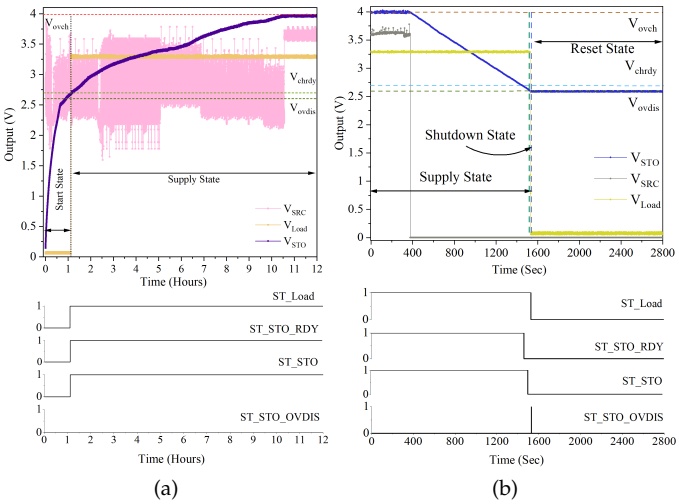

Fig. 10. (a) PMIC operating in start state and supply state after cold start during day hours (b) PMIC managing the power while the energy harvesting is stopped

The PMIC incorporates four status pins, namely ST_LOAD, ST_STO_RDY, ST_STO, and ST_STO_OVDIS, which serve the purpose of conveying crucial details regarding the operational states. The start state of the PMIC persists until the voltage at V_{STO} reaches the level of V_{chrdy}. Once this threshold is met, the PMIC transits into the supply state. Upon the rise of the voltage V_{STO} above V_{chrdy}, the status pin ST_STO_RDY has been asserted, indicating the successful transition of the PMIC into the supply state. Subsequently, V_{Load} reaches typical load voltage denoted as $V_{Load,Typ}$ which is approximately 3.23 V; thus ST_LOAD has been asserted showing that the PMIC is ready to deliver power to the sensor node. ST_STO is reset when V_{STO} goes below V_{ovdis} and asserted till V_{STO} surpasses V_{chrdy}. ST_STO_OVDIS is reset all the time, implying that the PMIC does not go to over-discharge state since V_{STO} does not get deplated below V_{ovdis}. The storage element takes approximately 10.5 hours to get fully charged, and V_{STO} approaches 4 V. Further, the PMIC ceases the delivery of power to the storage element as V_{STO} matches V_{ovch}. Although the PMIC undergoes cold start at 6 AM during the experimental duration, it is essential to note that the rate of charge of the storage element during this time is significantly lower compared to the period after 7 AM. The PMIC stays in supply state till V_{STO} is above V_{chrdy}, thus the sensor node can work uninterruptedly during this interval. Subsequently, the storage element is discharged at a constant current rate in order to examine the behaviour and operation states of the PMIC in short span of experimental duration. The result is shown in Fig. 10(b). V_{SRC} remains at 3.63 V till the source is providing power after which the discharge process starts and V_{STO} goes gradually down below V_{chrdy} i.e. 2.7 V thus, ST_STO_RDY is reset after that. Further, V_{STO} approaches V_{ovdis} which causes the PMIC to transit into shutdown state. As a result, ST_STO resets after this duration. The PMIC stays in shutdown state for 680 ms as per the manufacturer, and then it should go back to reset state. Experimentally ST_STO_OVDIS is asserted for 1 second, showing that the PMIC stays in shutdown state at this time. It stops delivering power to the sensor node further, which causes V_{Load} to be approximately 0.1 V.

3.4 Energy Harvesting

The system is deployed on field to comprehensively assess the energy harnessing capability of the hybrid energy harvesting sub-system. The primary objective of this investigation is to gain insights into the efficiency and reliability of this hybrid energy harvesting sub-system, thereby ensuring the energy sustainability. The measurement of accumulated energy has been conducted using ADM00805, which is a four-channel DC power monitoring evaluation board. Fig. 11 illustrates the amount of harvested energy by solar cell and TEG at different points in time.

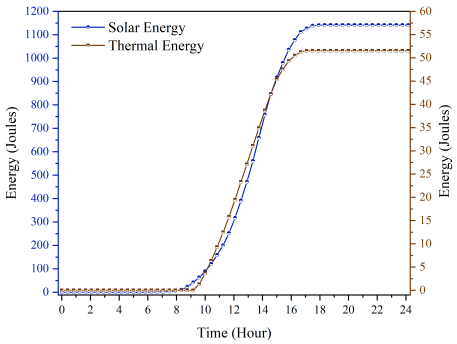

Fig. 11. Accumulated energy harvested from individual harvesters

The solar cell initiates the energy harvesting at approximately 6 AM, enabling the PMIC to undergo cold start. However, TEG can not start harvesting simultaneously due to insufficient ΔT. It commences harvesting energy after 9 AM when sunlight at intensity 27000 lux leads to the heating of the aluminum plate, resulting a discernible ΔT around two sides of TEG. Subsequently, Fig. 12 depicts the amount of total harvested energy throughout 24 hours period started at 12 AM.

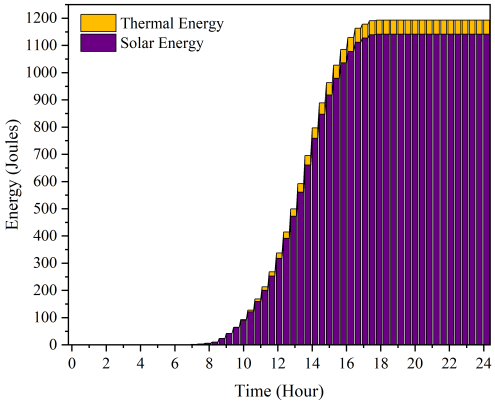

Fig. 12. Accumulated energy harvested from hybrid energy harvesting sub-system

The specific contributions from solar cell and the TEG in total accumulated energy by the hybrid energy harvesting sub-system can be observed from the same. The system harvests approximately 1200 J in 24 hours duration with average rate of 13.88 mW as per experimental observation. Further, it is essential to observe the sunlight intensity ($I_{Sunlight}$) and ΔT during various period of time as the amount of harvested energy primarily depends on these two parameters. Fig. 13 showcases the findings pertaining to this.

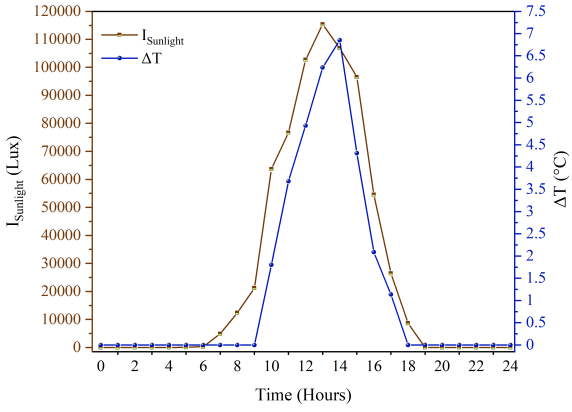

Fig. 13. Intensity of sunlight and ΔT accross the both sides of TEG during a day

Fig. 14 represents the amount of harvested energy during a complete day. It can be observed that the solar cell exhibits earlier energy harvesting than the TEG, as the aluminum plate takes time to get heated.

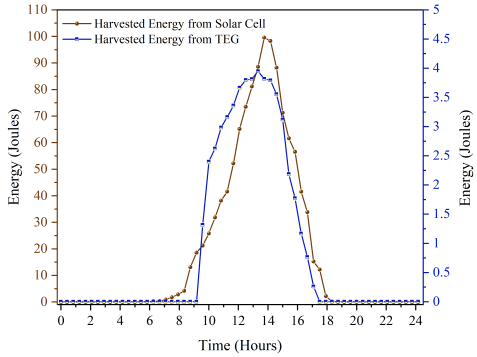

Fig. 14. Amount of harvested energy during a day through solar cell and TEG

3.5 Energy Consumption

The power consumption and energy consumption profile of the sensor node serve another considerable design aspect in achieving energy sustainability for the system. The current consumption of the components of the sensor node has been measured at 3.23 V using ADM00805 and NI-9203. The associated result has been presented in Table 2.

TABLE 2
Summery of Measured Current and Energy Consumption

Component	Peak Current	Average Current	Duration (Sec)		Energy		Mode
			Day	Night	Day	Night	
PIR Sensor	133 μA	124 μA	0	900	0	0.36 J	Active
	4.87 μA	3.17 μA	900	0	9.215 mJ	0	Sleep
Microcontroller	463 μA	488 μA	0.003	900	4.486 μJ	1.345 J	Active
	301 μA	345 μA	899.997	0	0.875 J	0	Sleep
Light Sensor	8.198 mA	62 μA	0.003		0.6μJ		Active
	33 μA	1.5 μA	899.997		4.36 mJ		Deep Sleep
LoRa	102.12 mA	70.67 mA	0	0.002	0	456.52 μJ	Active
	32 μA	8.5 μA	900	899.998	24.7 mJ	24.70 mJ	Deep Sleep
Total consumption (900 Sec)					0.904 J	1.734 J	—

The components of the system are critically selected by observing power requirements. These components are energy-efficient and can function in multiple modes. It can be observed that LoRa module is the most energy hungry component among others and it requires more than 90% of the total energy demand of the sensor node. Thus, the power consumption of the sensor node has been optimized using the proposed power-aware firmware. The summary of power consumption has been presented in Table 3. The significance of energy optimization can be comprehended from this.

TABLE 3
Summery of Power Consumption

	Parameters	LoRa	Sensor Node
Consumption before Optimization	Average Current	70.67 mA	77.53 mA
	Average Power	228.26 mW	250.42 mW
	Energy (1 Hours)	814.57 J	889.58 J
Optimized Power Consumption	Average Current	216 μA	603.53 μA
	Average Power	697.68 μW	1.95 mW
	Energy (1 Hours)	2.56 J	7.17 J

Fig. 15 presents the current consumption of the sensor node while the system is operating. It has been measured during a peculiar time period when the system was transitioning from day hour operation to full mode operation, which occurs specifically after sunset. It can be observed that after 180 seconds, there is a hike in current consumption. The average current consumption of the sensor node

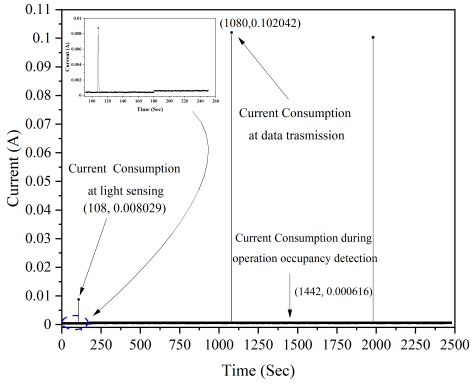

Fig. 15. Current consumption of the sensor node in 900 second operation cycle

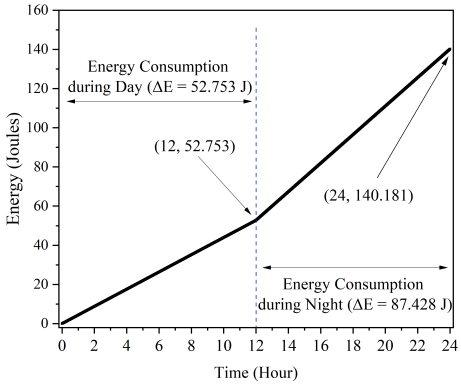

Fig. 16. Energy consumption of the sensor node in 24 hours

during day hours (I_{avg}^{day}) has been calculated as 335 μA. The same has been calculated during night (I_{avg}^{night}) as 597.157 μA. The average current consumption (I_{avg}) of different components of the sensor node is shown in Table 2. The energy consumption of the sensor node (E_{SN}) can be calculated using Eqn. (8).

$$E_{SN} = \frac{1}{T} \times [(E_{MCU}^{active} + E_{MCU}^{sleep}) + (E_{PIR}^{active} + E_{PIR}^{sleep}) + (E_{LoRa}^{active} + E_{LoRa}^{DS}) + (E_{LS}^{active} + E_{LS}^{DS})] \quad (8)$$

where E_{MCU}^{active} and E_{MCU}^{sleep} denote the energy consumption of the microcontroller in active and sleep mode, respectively. E_{PIR}^{active} and E_{PIR}^{sleep} represent the energy consumption associated with the PIR sensor during active and sleep mode, respectively. E_{LoRa}^{active} and E_{LoRa}^{DS} depict the energy consumption of LoRa in active mode and deep sleep mode, respectively. Energy consumption of light sensor during active mode and deep sleep mode have been represented by E_{LS}^{active} and E_{LS}^{DS}, respectively. The enery consumption of the sensor node has been theoretically calculated as 126.624 J in 24 hours duration. However, it is important to analyze the energy consumption of the sensor node during experimental conditions where the sensor node is exposed to different external conditions, such as temperature and humidity, which significantly affect the energy consumption. This can lead to a more realistic design. The energy consumption profile of the sensor node during 24 hours is presented in Fig. 16. It can be noted that the sensor node consumes 52.753 J with average power of 1.221 mW during day hours, and the same consumes 87.428 J with average power of 2.023 mW during night hours. Subsequently, it is worth noting that energy consumption during night exhibits a hike of approximately 66% compared to energy consumption during day. This is due radio communication, and continuous detection of occupancy with uninterrupted functioning of controller in active mode. Furthermore, the duty cycle of the operation has been calculated as 50% using the following expression considering the time period T as 900 seconds.

$$DutyCycle(\%) = \frac{T_{Active}}{T_{Active} + T_{Sleep}} \times 100 \quad (9)$$

where T_{Active} and T_{Sleep} represent the active time and sleep time of the sensor node, respectively.

3.6 Energy Sustainability

The system harvests energy with an average power of 13.88 mW, and the sensor node consumes average power (P_{avg}^{sn}) of 1.622 mW during a period of 24 hours. However, in order to ensure the energy sustainability of the system, there are two additional factors that need to be taken into consideration, which are power consumption of PMIC and leakage current of storage element. Both of these factors need to be minimum and optimized according to harvested power for achiving energy sustainability. Fig. 17 illustrates the self-discharge process of the lithium ion capacitor.

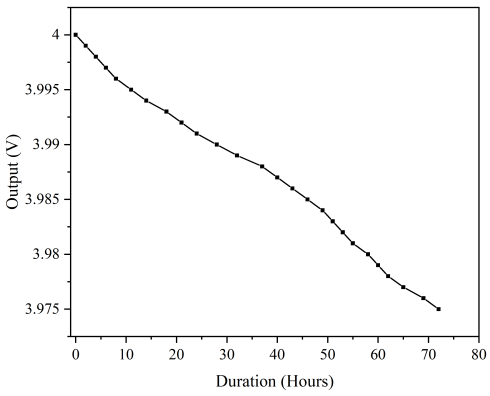

Fig. 17. Self-discharge of lithium-ion capacitor observed for a period of 72 hours

The lithium ion capacitor retained open circuit during 72 hours when the maximum temperature during day time is 42°C and the maximum Relative Humidity (RH) of 73%. The leakage current can be calculated as 14.467 μA using Eqn. (10).

$$I_{leakage} = \frac{C \times \Delta V}{\Delta T} \quad (10)$$

where C is denoted as the capacitance of the lithium-ion capacitor. ΔV is the change in the voltage level of the lithium-ion capacitor due to self-discharge, which is 0.025 V for this experiment. ΔT presents the total time taken in seconds, which is 259200 seconds in this case. The self-discharge over 72 hours accounts for 1.25% of the total harvested energy of the system in a day, rendering it practically insignificant. Further, the current consumption of the PMIC has been shown in Fig. 18. The average current and power

consumption of the PMIC has been observed as 230.804 μA and 466.317 μW, respectively at 2.021 V implying the average power consumption of the system (P_{sys}) as 2.489 mW during night hours and 1.687 mW during day hours, respectively. P_{sys} can be calculated as 2.088 mW cosidering 24 hours operation cycle. Furthermore, the system has been deployed on field, and the charging and discharging profile of the lithium-ion capacitor has been measured.

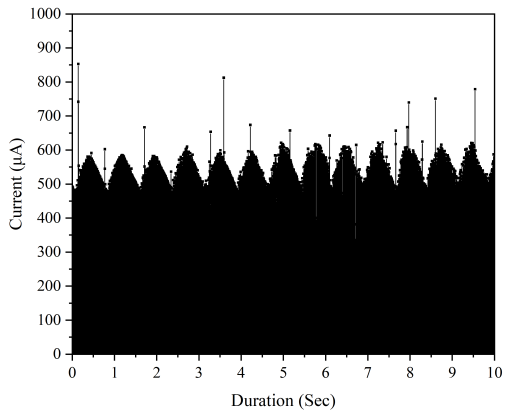

Fig. 18. Current consumption of PMIC at 2.02 V supply

Fig. 19 presents the voltage profile of the lithium-ion capacitor (V_{lic}) observed for 7 days. The charging process commences on the initial day, starting from 0 V, and persists until the system successfully harnesses energy from the designated source. The charging continues for approximately 12 hours, and V_{lic} reaches approximately 3.88 V. It has been experimentally observed that the sensor node starts operating after the V_{lic} exceeds V_{chrdy} 2.7 V since the PMIC starts supplying a minimum of 3.2 V to the sensor node afterwards. Though the sensor node executes the assigned tasks with average power consumption of 1.22 mW, V_{lic} exhibits an increasing trend during the day hours. This is because the system can harvest energy with higher average power of 26.136 mW during day hours enabling the PMIC to supply power to the sensor node and simultaneously charge the lithium-ion capacitor.

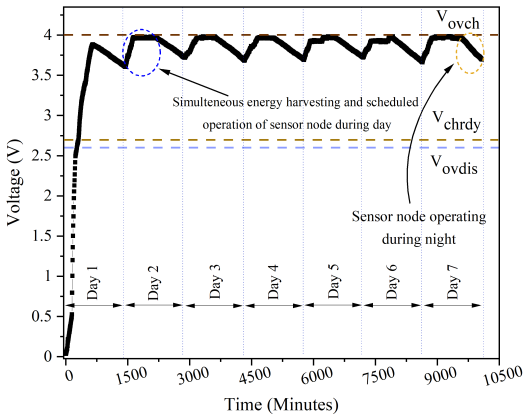

Fig. 19. Charging and discharging profile of lithium-ion capacitor

The sensor node turns on the street light and starts operating its scheduled task, which are supposed to occur during night hours with average power consumption of 2.023 mW. It can be noted that the PMIC consumes energy from the harvesters during day hours, and depends on the storage element for power in the absence of energy from the harvesters. The total energy consumption of the PMIC during 24 hours has been empirically calculated as 40.28 J. V_{lic} thus decreases from 3.88 V to 3.6 V during the night hours of the first day. Further, it starts harvesting energy, taking 4 to 6 hours starting at 6 AM to completely charge the lithium-ion capacitor at 4 V in subsequent days. V_{lic} gets depleted from 4 V to maximum 3.69 V during night. This ensures the uninterrupted operation of the system, featuring it with energy sustainability. The runtime of the system (T_{run}) can be calculated as using the following expression.

$$T_{run} = \frac{0.5 \times C_{lic}({V_{lic}}^2 - {V_{chrdy}}^2)}{E_{system}} \tag{11}$$

where C_{lic} denotes capacitance of the lithium-ion capacitor, respectively. E_{system} is the amount of energy that the sensor node along with that of PMIC drag from the lithium-ion capacitor, calculated as 160.32 J. The runtime is calculated as more than 3 days once the lithium-ion capacitor is fully charged to 4 V. This implies that the system can sustain for more than 3 days in complete absence of energy.

3.7 Performance Evaluation and Comparative Analysis

3.7.1 Performance Evaluation

The performance of bSlight 2.0 has been comprehensively evaluated based on few factors. Communication has great impact on performance of any WSN and IoT enabled device. The proposed system supports long-range communication through integration of LoRaWAN technology. Certain parameters have been carefully considered while implementing LoRaWAN to ensure seamless wireless communication. It should be noted that the parameters have been set as per the application requirement and to uphold high QoS. The device exhibits maximum communication range of up to 1.1 KM. On the other hand, Packet Delivery Rate (PDR) is significantly impacted by communication range, and it is essential to maintain PDR as high as possible to ensure the QoS to remain high. PDR gets below 90% in case the communication range exceeds 761 meters; thus the gateway has been placed at a distance of 761 meters from the end node. Further, communication delay plays a vital role in determining the QoS of the system. The data size requiring transmission amounts to 5 bytes; consequently, a simulation has been conducted using an online tool to ascertain the Time on Air (ToA) across different Spreading Factors (SF). The power consumption of the device increases with increase in SF and bandwidth.

Thus, the SF has been kept minimum at 7 to ensure low power consumption during consumption, which is the primary focus of this work. ToA for SF 7 has been determined as approximately 31 ms, which is considered reasonable since the communication interval is 900 seconds. Though high bandwidth results in faster transmission, it also consumes more power on the other hand. Thus, the

TABLE 4
Comparison of state-of-the-art Smart Street Light Management Systems

References	Radio Technology	Sensing Parameters	Wireless Range	Average Power Consumption of Sensor node	Energy Storage	Energy Sustainability	Power Optimization Technique
Kaleem *et al.*, 2016 [8]	ZigBee	Power, Light intensity, Motion	Short	384 mW*	N/A	No	No
Shahzad *et al.*, 2016 [9]	ZigBee	Light intensity, Temperature, Power	Short	414 mW*	N/A	No	No
Bellido-Outeiriño *et al.*, 2016 [15]	ZigBee	Motion	Short	—	N/A	No	No
Daely *et al.*, 2017 [10]	ZigBee	Humidity, Power, Particle Concentration	Short	4.13 W*	N/A	No	No
Chen *et al.*, 2018 [21]	NB-IoT	Temperature, Humidity, Light intensity, and Power	Long	218 mW*	Battery	No	No
Abdullah *et al.*, 2018 [12]	N/A	Motion and Light intensity	N/A	387 mW*	Battery	No	No
Saha *et al.*, 2021 [11]	WiFi	Temperature, Humidity, Rain Motion and Light intensity	Long	692.4 mW*	N/A	No	No
Sorif *et al.*, 2021 [13]	WiFi	Motion and Light intensity	Long	525 mW*	N/A	No	No
Sanchez-Sutil *et al.*, 2021 [14]	LoRaWAN	Motion, Current, Voltage	Long	—	N/A	No	No
N. Valov *et al.*, 2023 [36]	WiFi	Motion, Light intensity	Long	211.37 mW	N/A	No	No
Proposed work (bSlight 2.0)	LoRaWAN	Motion, Light intensity	Long	**1.662 mW**	**Lithium-ion capacitor and capacitor**	**Yes**	**Duty cycle**

*The original manuscript lacks information regarding the power consumption of the sensor node. The value is calculated analysing the publicly accessible datasheets of the components, for comparison purpose. N/A depicts that the component is unavailable in this work. '—' indicates that niether direct nor relevant data for calculation is available in the original manuscript.

TABLE 5
Comparison with State-of-the-art LoRaWAN based Solar Energy or Artificial Light Energy Powered Energy Autonomous Devices

References	Energy Source	Size of Harvester (mm^2)	Harvester Output	Storage	Application	Power Consumption	Current Consumption	Duty Cycle (%)
Wu *et al.*, 2018 [30]	Solar & Artificial light	2826.9	90 mW	Supercapacitor	Environmental parameter monitoring	—	75.57 μA – 1.38 mA	15.16
Zhang *et al.*, 2019 [39]	Solar	—	10 W	Battery	Soil health monitoring	—	—	—
Sadowski *et al.*, 2020 [42]	Solar	28900	3.65 W	Battery	Soil health monitoring	29.33 mW	—	—
Bhusal *et al.*, 2020 [40]	Solar & Artificial light	23730	3.5 W	Battery	Air qualty monitoring	25.9 mW	7 mA	0.16
Ali *et al.*, 2021 [43]	Solar	—	3 W	Battery	Air pollution monitoring	$\approx$ 14.306 mW – 14.97 mW	—	$\approx$ 5 – 6
Ramson *et al.*, 2021 [28]	Solar	4550	350 mW	Battery	Soil health monitoring	—	13 mA	1.65
Kombo *et al.*, 2021 [41]	Solar	—	6 W	Battery	Under groundwater monitoring	104.081 mW	—	< 1
Petrariu *et al.*, 2021 [44]	Solar	—	330 mW	Battery and Supercapacitor	Environmental parameter monitoring and Geolocation tracking	—	1.69 mA	2.66
Yuksel *et al.*, 2021 [45]	Solar	—	1 W	Supercapacitor	Environmental parameter monitoring	380 mW	—	—
Ramson *et al.*, 2022 [29]	Solar	4550	350 mW	Battery	Smart trashbin	—	1.5 mA	2.73
Mohanty *et al.*, 2023 (bSlight) [6]	Solar & Artificial light	2368	66 mW	Supercapacitor	Street light managemenet	2.023 mW	619.14 μA	50
Proposed Work (bSlight 2.0)	**Solar & Solar Thermal**	2486	**182.35 mW**	**Lithium-ion capacitor and Capacitor**	Street light managemenet	2.088 mW	827.96 μA	50

'—' indicates that neither direct nor relevant data for calculation is provided in the original publication.

TABLE 6
Comparision with state-of-the-art Energy Autonomous/Self-Powered Street Light Management System

References	Energy Source	Numer of Harvesters	Maximum Output Power of Harvesters	Size of Harvesters	Battery-free design framework	Power Consumption of Sensor Node	Duty Cycle	Power Consumption of System	Number of of PMIC(s)	Energy Storage	MCU Architecture	PCB Size	System Footprint (cm)
Mohanty *et al.*, 2020 [7]	Solar	1	1.5 W	10611 mm^2	No	42.94 mW	N/A	—	1	Battry	AVR	—	—
Mohanty *et al.* (bSlight), 2024 [6]	Solar & Artificial light	1	66 mW	2368 mm^2	Yes	1.983 mW	50%	2.022 mW	2	Supercapacitor	ARM Cortex M0	3750 mm^2	12.5 x 8.5 x 2.5
Proposed Work (bSlight 2.0)	**Solar & Solar Thermal**	**2**	**182.35 mW**	2486 mm^2	Yes	**1.662 mW**	50%	2.088 mW	1	**Lithium-ion capacitor & capacitor**	**ARM Cortex M4**	**3120** mm^2	**10.5 x 6.5 x 2.3**

bandwidth of LoRaWAN has been fixed at 125 KHz, considering the communication interval and size of the data. The system operates in real-time with 50% of duty cycle. It has been tested on field for more than 30 days for validating its real-time operation capability and the tasks are found to be working adhering particular deadline. The power consumption of bSlight 2.0 has been optimized to 2.088 mW, which is lowest in state-of-the-art street light management systems. Most of the commercially available off-the-shelf components have life span ranging from 5 to 10 years. Though the lifetime expectancy of bSlight 2.0 is influenced by several factors, with the primary determining factor being the lifespan of the lithium-ion capacitor. Its lifetime can be empirically determined to ensure it does not fall below 10 years. Thus, E_{system} has to be considered, which is reported as 160.32 J. It exhibits 50000 charge cycles when subjected to a storage temperature of 23°C to 27°C, the discharge current of 20 C-Rate, and Depth of Discharge (DOD) of 100% as per the specification provided by the manufacturer. The average ambient temperature of the place where the system has been tested is 25.9°C, 20C rating allows sensor node to drag 1.6 A current safely, and the sensor node almost uses 100% DOD in this work. Based on the aforementioned considerations, the lifetime can be empirically calculated following method descirbed in [38] as 1024.65 years, which seems unrealistic in practical terms. Thus, the proposed device can be considered to have an operational lifetime of minimum 5 to 10 years, which is adequate to deploy it on field.

3.7.2 Comparision with State-of-the-art Solutions

The proposed system has been thoroughly evaluated and compared against existing state-of-the-art street light management systems, as depicted in Table 4. A comparative analysis is also presented in Table 5 to assess the advancements achieved compared to the state-of-the-art energy-autonomous devices. The presented works are energy harvesting enabled LoRaWAN based systems proposed for various applications. These systems commonly harvest energy from direct sunlight. The comprehensive enhancements attained in this work have been succinctly summarized and outlined as follows.

- In continuation to the state-of-the-art street light management systems, the proposed system manages the operation of street light aiming to reduce energy budget. The novelty of the work lies in adding energy sustainability to the management system.
- It is a hybrid solar and solar thermal energy powered, energy-autonomous, batteryless, IoT enabled device working in real-time, achieving maximum percentage of duty cycle i.e. 50% among state-of-the-art LoRaWAN based energy-autonomous systems. Though the duty-cycle percentage is higher, the total size of the harvesters is the minimum as 2486 mm^2.
- The power consumption of the sensor node is 1.662 mW which is reported as minimal among state-of-the-art street light management systems.

In order to comprehensively assess the merits of the proposed system, it is imperative to compare it with our previously developed energy autonomous system for street light management. Table 6 shows the comparative analysis, which can summarize the advantages offered by the proposed work in contrast to our earlier designs. The advantages are outlined below.

- The proposed work aims to integrate a hybrid energy harvesting scheme combining solar and solar thermal energy. In contrast, the viability of energy harvesting from artificial light has been explored in [6], which is used as the primary energy source for the device.
- The proposed device requires 37.63% of total energy harvested during 24 hours to execute the desired task during day hours when energy availability is easy and high in outdoor condition, specifically at an average harvesting power of 27.77 mW, and the same needs 62.36% of energy for executing the desired task during night hours when energy availability is extremely critical. Although the system designed in [6] can harvest energy from sunlight when the harvester harvests energy at 36.98 mW; the harvested energy can not be effectively stored for powering the sensor node during night due to low energy density of supercapacitor which is a major limitation. Instead, it has been designed to harvest energy during night when the harvester can harvest energy in the range of 3.2 mW to 6.4 mW. Thus, the device requires uninterrupted power from the harvester irrespective of time to run the sensor node. However, inconvenience weather conditions such as heavy rain, and dense fog may restrict the energy harvesting from artificial light causing power failure to the system in real-time testbed.
- In order to address the aforementioned limitation, this work proposes an alternative approach that focuses on harnessing energy from solar and solar thermal energy during day hours when energy availability is high and can be harnessed without introducing much manufacturing cost and design complicacy.
- The device integrates a single PMIC to manage the energy in the system effectively. It can simultaneously store the harnessed energy and power the sensor node exhibiting efficient power management. Lithium-ion capacitor has been used as an energy storage element which provides the flexibility to the device to sustain during adverse conditions when energy harvesting is critical. In addition, the implementation of a single PMIC for energy management has provided the advantage of reducing the number of components implying less maintenance requirement and device footprint. Furthermore, the average power consumption of the system is approximately 4% higher compared to [6]; nevertheless, it is important to acknowledge that the harvesters in the proposed design exhibit higher power generation capability in comparison to the aforementioned work, permitting the implementation of a single PMIC with bit higher energy consumption.

4 Conclusion

A hybrid solar and solar thermal energy powered batteryless, low-power, sustainable street light management system has been proposed for remote areas of India such as villages, hilly regions, and deserts. The system has been retrofitted with an existing LED street light in order to validate its feasibility in real-time testbed. It uses a small monocrystalline type solar cell of dimension 42 mm x 23 mm and a TEG of dimension 42 mm x 38 mm to harness energy from sunlight and thermal energy generated due to sunlight. A dual energy storage unit including 150 F lithium-ion capacitor and 300 μF capacitor has been implemented with the help of an off-the-shelf, highly versatile, buck-boost PMIC. It ensures efficient energy harvesting with the help of built-in MPPT and smart energy management algorithm that allows charging the storage element and simultaneously powering the sensor node with average power consumption of 466.317 μW at 2.02 V. The system controls the illuminance of the street light according to vehicular and pedestrian movement around the road which can help reducing energy budget of street light. It also helps the admin to find the faulty street lights through remote monitoring. LoRaWAN has been incorporated for long range communication, which exhibits communication range of up to 761 m in practical scenario. The sensor node works in 50% duty cycle with average power consumption of 1.662 mW at 3.23 V supply voltage.

In future, security problems may potentially be addressed by the use of hardware mechanisms developed in [37], [46]. The number of tasks can be scheduled through implementation of AI technology [47], [48].

References

[1] S. P. Mohanty, U. Choppali and E. Kougianos, "Everything you wanted to know about smart cities: The Internet of things is the backbone," *IEEE Consumer Electronics Magazine*, vol. 5, no. 3, pp. 60-70, July 2016, doi: 10.1109/MCE.2016.2556879.

[2] "Global IoT and non-IoT connections 2010-2025 — Statista," *Statista*, Sep. 06, 2022. https://www.statista.com/statistics/1101442/iot-number-of-connected-devices-worldwide/#statisticContainer

[3] "Sustainable Development Goals," *UNDP*. [Online]. Available: https://www.undp.org/sustainable-development-goals.

[4] G. Scandurra, A. Arena, and C. Ciofi, "A Brief Review on Flexible Electronics for IoT: Solutions for Sustainability and New Perspectives for Designers", *Sensors*, vol. 23, no. 11, pp. 5264-5395, Jun. 2023, doi: 10.3390/s23115264.

[5] Y. He, X. Cheng, W. Peng, and G. L. Stuber, "A survey of energy harvesting communications: models and offline optimal policies," *IEEE Commun. Mag.*, vol. 53, no. 6, pp. 79–85, Jun. 2015, doi: 10.1109/MCOM.2015.7120021.

[6] P. Mohanty, U. Pati, K. Mahapatra and S. Mohanty, "bSlight: Battery-Less Energy Autonomous Street Light Management System for Smart City" *IEEE Transactions on Sustainable Computing*, vol. 9, no. 01, pp. 100-114, 2024, doi: 10.1109/TSUSC.2023.3310884

[7] P. Mohanty, U. C. Pati, and K. Mahapatra, "Self-Powered Intelligent Street Light Management System for Smart City," in *Proc. IEEE 18th India Council International Conference (INDICON)*, Dec. 2021, pp. 1-6, doi:10.1109/INDICON52576.2021.9691575.

[8] Z. Kaleem, T. M. Yoon, and C. Lee, "Energy Efficient Outdoor Light Monitoring and Control Architecture Using Embedded System," *IEEE Embedded Syst. Lett.*, vol. 8, no. 1, pp. 18–21, Mar. 2016, doi: 10.1109/LES.2015.2494598.

[9] G. Shahzad, H. Yang, A. W. Ahmad, and C. Lee, "Energy-Efficient Intelligent Street Lighting System Using Traffic-Adaptive Control," *IEEE Sensors J.*, vol. 16, no. 13, pp. 5397–5405, Jul. 2016, doi: 10.1109/JSEN.2016.2557345.

[10] P. T. Daely, H. T. Reda, G. B. Satrya, J. W. Kim, and S. Y. Shin, "Design of Smart LED Streetlight System for Smart City With Web-Based Management System," *IEEE Sensors J.*, vol. 17, no. 18, pp. 6100–6110, Sep. 2017, doi: 10.1109/JSEN.2017.2734101.

[11] D. Saha, S. M. Sorif, and P. Dutta, "Weather Adaptive Intelligent Street Lighting System With Automatic Fault Management Using Boltuino Platform," in *Proc. International Conference on ICT for Smart Society (ICISS)*, Aug. 2021, pp. 1–6, doi: 10.1109/ICISS53185.2021.9533234.

[12] A. Abdullah, S. H. Yusoff, S. A. Zaini, N. S. Midi, and S. Y. Mohamad, "Smart Street Light Using Intensity Controller," in *Proc. 7th International Conference on Computer and Communication Engineering (ICCCE)*, Sep. 2018, pp. 1–5, doi: 10.1109/ICCCE.2018.8539321.

[13] S. M. Sorif, D. Saha, and P. Dutta, "Smart Street Light Management System with Automatic Brightness Adjustment Using Bolt IoT Platform," in *Proc. IEEE International IOT, Electronics and Mechatronics Conference (IEMTRONICS)*, Apr. 2021, pp. 1–6, doi: 10.1109/IEMTRONICS52119.2021.9422668.

[14] F. Sanchez-Sutil and A. Cano-Ortega, "Smart regulation and efficiency energy system for street lighting with LoRa LPWAN," *Sustainable Cities and Society*, vol. 70, pp. 102912-102927, Jul. 2021, doi: 10.1016/j.scs.2021.102912.

[15] F. Bellido-Outeiriño, F. Quiles-Latorre, C. Moreno-Moreno, J. Flores-Arias, I. Moreno-García, and M. Ortiz-López, "Streetlight Control System Based on Wireless Communication over DALI Protocol," *Sensors*, vol. 16, no. 5, pp. 597–619, Apr. 2016, doi: 10.3390/s16050597.

[16] N. Saokaew, N. Kitsatit, T. Yongkunawut, P. N. Ayudhya, E. Mujjalinvimut, T. Sapaklom, P. Aregarot, and J. Kunthong, "Smart Street Lamp System using LoRaWAN and Artificial Intelligence PART I," in *Proc. 9th International Electrical Engineering Congress (iEECON)*, Mar. 2021, pp. 189–192, doi: 10.1109/iEECON51072.2021.9440337.

[17] F. Leccese, "Remote-Control System of High Efficiency and Intelligent Street Lighting Using a ZigBee Network of Devices and Sensors," *IEEE Trans. Power Delivery*, vol. 28, no. 1, pp. 21–28, Jan. 2013, doi: 10.1109/TPWRD.2012.2212215.

[18] F. Leccese, M. Cagnetti, and D. Trinca, "A Smart City Application: A Fully Controlled Street Lighting Isle Based on Raspberry-Pi Card, a ZigBee Sensor Network and WiMAX," *Sensors*, vol. 14, no. 12, pp. 24408–24424, Dec. 2014, doi: 10.3390/s141224408.

[19] L. Yongsheng, L. Peijie, and C. Shuying, "Remote Monitoring and Control System of Solar Street Lamps Based on ZigBee Wireless Sensor Network and GPRS," in *Electronics and signal processing*, 2011, pp. 959–967.

[20] R. Kodali, and S. Yerroju, "Energy efficient smart street light," in *Proc. 3rd International Conference on Applied and Theoretical Computing and Communication Technology (iCATccT)*, Dec. 2017, pp. 190–193, doi: 10.1109/ICATCCT.2017.8389131.

[21] S. Chen, G. Xiong, J. Xu, S. Han, F.-Y. Wang, and K. Wang, "The Smart Street Lighting System Based on NB-IoT," in *Proc. Chinese Automation Congress (CAC)*, Nov. 2018, pp. 1196–1200, doi: 10.1109/CAC.2018.8623281.

[22] Y. -S. Yang, S. -H. Lee, G. -S. Chen, C. -S. Yang, Y. -M. Huang and T. -W. Hou, "An Implementation of High Efficient Smart Street Light Management System for Smart City," *IEEE Access*, vol. 8, pp. 38568-38585, Feb. 2020, doi: 10.1109/ACCESS.2020.2975708.

[23] C. -T. Lee, L. -B. Chen, H. -M. Chu and C. -J. Hsieh, "Design and Implementation of a Leader-Follower Smart Office Lighting Control System Based on IoT Technology," *IEEE Access*, vol. 10, pp. 28066-28079, 2022, doi: 10.1109/ACCESS.2022.3158494.

[24] M. Abdolhosseini and R. Abdollahi, "Designing and Implementing a Lighting Control System Based on Constrained Info-Fuzzy, to Save Energy and Satisfy Users," *IEEE Transactions on Industrial Informatics*, doi: 10.1109/TII.2024.3353917.

[25] S. Bandopadhaya, R. Dey, and A. Suhag, "Integrated healthcare monitoring solutions for soldier using the internet of things with distributed computing," *Sustainable Computing: Informatics and Systems*, vol. 26, pp. 100378-100384, Jun. 2020, doi: 10.1016/j.suscom.2020.100378.

[26] P. Kumari, R. Mishra, H. P. Gupta, T. Dutta and S. K. Das, "An Energy Efficient Smart Metering System Using Edge Computing in LoRa Network," *IEEE Transactions on Sustainable Computing*, vol. 7, no. 4, pp. 786-798, Oct. 2022, doi: 10.1109/TSUSC.2021.3049705.

[27] S. Vishnu, S. R. J. Ramson, S. Senith, T. Anagnostopoulos, A. M. Mahfouz, X. Fan, S. Srinivasan, and A. Kirubaraj, "IoT-Enabled Solid Waste Management in Smart Cities," *Smart Cities*, vol. 4, no. 3, pp. 1004–1017, Jul. 2021, doi: 10.3390/smartcities4030053.

[28] S. R. J. Ramson, W. D. León-Salas, Z. Brecheisen, E. J. Foster, C. T. Johnston, D. G. Schulze, T. Filley, R. Rahimi, M. J. C. V. Soto, J. A. L. Bolivar, and M. P. Málaga, "A Self-Powered, Real-Time, LoRaWAN IoT-Based Soil Health Monitoring System," *IEEE Internet of Things Journal*, vol. 8, no. 11, pp. 9278-9293, Jun. 2021, doi: 10.1109/JIOT.2021.3056586.

[29] S. R. J. Ramson, S. Vishnu, A. A. Kirubaraj, T. Anagnostopoulos and A. M. Abu-Mahfouz, "A LoRaWAN IoT-Enabled Trash Bin Level Monitoring System," *IEEE Transactions on Industrial Informatics*, vol. 18, no. 2, pp. 786-795, Feb. 2022, doi: 10.1109/TII.2021.3078556.

[30] F. Wu, J. M. Redoute, and M. R. Yuce, "WE-Safe: A Self-Powered Wearable IoT Sensor Network for Safety Applications Based on LoRa," *IEEE Access*, vol. 6, pp. 40846–40853, 2018, doi: 10.1109/ACCESS.2018.2859383.

[31] S. Suman and S. De, "Low Complexity Dimensioning of Sustainable Solar-Enabled Systems: A Case of Base Station," *IEEE Trans. on Sustainable Computing*, vol. 5, no. 3, pp. 438-454, Jul. 2020, doi: 10.1109/TSUSC.2019.2947642.

[32] MNRE, "Brief on Off-grid Solar PV Programme" [Online]. Available: https://mnre.gov.in/solar-off-grid/

[33] A. H. Dehwah, M. Mousa, and C. G. Claudel, "Lessons learned on solar powered wireless sensor network deployments in urban, desert environments," *Ad Hoc Networks*, vol. 28, pp. 52–67, May 2015, doi: 10.1016/j.adhoc.2015.01.013.

[34] M. V. Ramesh, "Design, development, and deployment of a wireless sensor network for detection of landslides," *Ad Hoc Networks*, vol. 13, pp. 2–18, Feb. 2014, doi: 10.1016/j.adhoc.2012.09.002.

[35] e-peas semiconductor. *Highly Versatile, Regulated Single-Output, Buck-Boost Ambient Energy Manager For Up to 7-cell Solar Panels*. Accessed: Oct. 2023. [Online]. Available: https://e-peas.com/product/aem10330/.

[36] N. Valov *et al.*, "Design of a Smart System for Street Light Monitoring and Control," in *Proc. 7th International Symposium on Multidisciplinary Studies and Innovative Technologies (ISMSIT)*, 2023, pp. 1-4, doi: 10.1109/ISMSIT58785.2023.10304998.

[37] S. K. Ram, S. R. Sahoo, B. B. Das, K. Mahapatra and S. P. Mohanty, "Eternal-Thing: A Secure Aging-Aware Solar-Energy Harvester Thing for Sustainable IoT," *IEEE Transactions on Sustainable Computing*, vol. 6, no. 2, pp. 320-333, Apr. 2021, doi: 10.1109/TSUSC.2020.2987616.

[38] Electropedia, "Battery and Energy Technologies," *mpoweruk.com*. [Online]. Available: https://www.mpoweruk.com/life.htm#:~:text=This%20is%20because%20battery%20life,100%20cycles%20at%201%25%20DOD. [Accessed: Dec. 20, 2021].

[39] X. Zhang, M. Zhang, F. Meng, Y. Qiao, S. Xu and S. Hour, "A Low-Power Wide-Area Network Information Monitoring System by Combining NB-IoT and LoRa," *IEEE Internet of Things Journal*, vol. 6, no. 1, pp. 590-598, Feb. 2019, doi: 10.1109/JIOT.2018.2847702.

[40] H. Bhusal, P. Khatiwada, A. Jha, J. Soumya, S. Koorapati and L. R. Cenkeramaddi, "A Self-Powered Long-range Wireless IoT Device based on LoRaWAN," in *Proc. IEEE International Symposium on Smart Electronic Systems (iSES) (Formerly iNiS)*, 2020, pp. 242-245, doi: 10.1109/iSES50453.2020.00061.

[41] O. H. Kombo, S. Kumaran and A. Bovim, "Design and Application of a Low-Cost, Low- Power, LoRa-GSM, IoT Enabled System for Monitoring of Groundwater Resources With Energy Harvesting

Integration," *IEEE Access*, vol. 9, pp. 128417-128433, 2021, doi: 10.1109/ACCESS.2021.3112519.
[42] S. Sadowski, and P. Spachos, "Wireless technologies for smart agricultural monitoring using internet of things devices with energy harvesting capabilities," *Computers and Electronics in Agriculture*, vol. 172, pp. 103558-103566, Mar. 2020, doi: 10.1016/j.compag.2020.105338.
[43] S. Ali, T. Glass, B. Parr, J. Potgieter and F. Alam, "Low Cost Sensor With IoT LoRaWAN Connectivity and Machine Learning-Based Calibration for Air Pollution Monitoring," *IEEE Transactions on Instrumentation and Measurement*, vol. 70, pp. 1-11, 2021, doi: 10.1109/TIM.2020.3034109.
[44] A. I. Petrariu, A. Lavric, E. Coca and V. Popa, "Hybrid Power Management System for LoRa Communication Using Renewable Energy," *IEEE Internet of Things Journal*, vol. 8, no. 10, pp. 8423-8436, May 2021, doi: 10.1109/JIOT.2020.3046324.
[45] M. Yuksel, and H. Fidan, "Energy-aware system design for batteryless LPWAN devices in IoT applications," *Ad Hoc Networks*, vol. 122, pp. 102625-102645, Jul. 2021, doi: 10.1016/j.adhoc.2021.102625.
[46] S. K. Ram, S. R. Sahoo, B. B. Das, K. K. Mahapatra, and S. P. Mohanty, "Eternal-Thing 2.0: Analog-Trojan Resilient Ripple-Less Solar Harvesting System for Sustainable IoT," *ACM Journal on Emerging Technologies in Computing Systems (JETC)*, vol. 19, no. 2, pp. 1-25, Mar. 2023, doi: 10.1145/3575800.
[47] C. S. Sandeep, P. Mohanty and U. C. Pati, "Machine Learning Based Framework for Prediction of Photovoltaic Output Power," *Proc. IEEE 3rd International Conference on Sustainable Energy and Future Electric Transportation (SEFET)*, Aug. 2023, pp. 1-6, doi: 10.1109/SeFeT57834.2023.10245655.
[48] P. Mohanty, U. C. Pati, and K. Mahapatra, "Deep Learning Based Framework for Forecasting Solar Panel Output Power," in *Proc. IFIP advances in information and communication technology*, Oct. 2023, pp. 1-19, doi: 10.1007/978-3-031-45878-1_16.

Prajnyajit Mohanty (Graduate Student Member, IEEE) received B.Tech degree in Electronics and Instrumentation Engineering from National Institute of Science and Technology, Berhampur, in 2017, and M.Tech degree in Control and Instrumentation Engineering from Veer Surendra Sai University of Technology, Burla, in 2019. He is currently pursuing Ph. D. in Electronics and Communication Engineering from National Institute of Technology Rourkela. His research interests include Energy Harvesting Systems, Internet of Things, Low Power Embedded System Design, and Machine Learning.

Umesh C. Pati (Senior Member, IEEE) is a full Professor at the Department of Electronics and Communication Engineering, National Institute of Technology (NIT), Rourkela. He has obtained his B.Tech. degree in Electrical Engineering from NIT, Rourkela, Odisha. He received both M.Tech. and Ph.D. degrees in Electrical Engineering with specialization in Instrumentation and Image Processing respectively from IIT, Kharagpur. His current areas of interest are Image/Video Processing, Computer Vision, Artificial Intelligence, Internet of Things (IoT), Industrial Automation, and Instrumentation Systems. He has authored/edited two books and published over 100 articles in the peer-reviewed international journals as well as conference proceedings. He is a Fellow of The Institution of Engineers (India), and Institution of Electronics and Telecommunication Engineers (IETE). He is also life member of various professional bodies like MIR Labs (USA), Indian Society for Technical Education, Computer Society of India, Instrument Society of India and Odisha Bigyan Academy.

Kamalakanta Mahapatra (Senior Member, IEEE) Dr. Kamalakanta Mahapatra is a Professor (HAG) in Electronics and Communication Engineering Department of National institute of Technology, Rourkela. He assumed professor position since February 2004. He obtained his B. Tech degree with Honours from Regional Engineering College, Calicut in 1985, Master's from Regional Engineering College, Rourkela in 1989 and Ph. D. from IIT Kanpur in 2000. He is a senior member of the IEEE and a fellow of the institution of Engineers (India) in ECE Division. Presently , he is the Chairman of IEEE Rourkela Sub-section and mentor of IEEE CTSoC chapter of Kolkata section. He has published several research papers in National and International Journals. He received coveted J. C. Bose award for best engineering oriented research in the year 2014. His research interests include Embedded Computing Systems, VLSI Design, Hardware Security and Industrial/Consumer/Power Electronics. He has supervised 24 PhD dissertations and 92 Master's theses.

Saraju P. Mohanty (Senior Member, IEEE) received the bachelor's degree (Honors) in electrical engineering from the Orissa University of Agriculture and Technology, Bhubaneswar, in 1995, the master's degree in Systems Science and Automation from the Indian Institute of Science, Bengaluru, in 1999, and the Ph.D. degree in Computer Science and Engineering from the University of South Florida, Tampa, in 2003. He is a Professor with the University of North Texas. His research is in "Smart Electronic Systems" which has been funded by National Science Foundations (NSF), Semiconductor Research Corporation (SRC), U.S. Air Force, IUSSTF, and Mission Innovation. He has authored 500 research articles, 5 books, and invented 10 granted/pending patents. His Google Scholar h-index is 57 and i10-index is 243 with 13,000 citations. He is a recipient of 19 best paper awards, Fulbright Specialist Award in 2021, IEEE Consumer Electronics Society Outstanding Service Award in 2020, the IEEE-CS-TCVLSI Distinguished Leadership Award in 2018, and the PROSE Award for Best Textbook in Physical Sciences and Mathematics category in 2016. He has delivered 24 keynotes and served on 14 panels at various International Conferences. He has been the Editor-in-Chief of the IEEE Consumer Electronics Magazine during 2016-2021 and currently serves on the editorial board of 8 journals/transactions. He has mentored 3 post-doctoral researchers, and supervised 15 Ph.D. dissertations, 27 M.S. theses, and 27 undergraduate senior-projects.